

A Catalog of Absorption Lines in Eight HST/STIS E230M 1.0 < z < 1.7 Quasar Spectra ^{*}

N. Milutinović,^{1,2} T. Misawa,¹ R. S. Lynch,^{1,3} J. R. Masiero,^{1,4} C. Palma,¹ J. C. Charlton,¹
D. Kirkman,⁵ S. Bockenhauer⁵ and D. Tytler⁵

¹ Department of Astronomy & Astrophysics, 525 Davey Lab, Pennsylvania State University, University Park, PA 16802

² Department of Physics & Astronomy, University of Victoria, Elliott Building, 3800 Finnerty Rd, Victoria, BC, V8P 5C2 Canada

³ Department of Astronomy, P.O. Box 400325, University of Virginia, Charlottesville, VA 22904

⁴ Institute for Astronomy, University of Hawaii 2680 Woodlawn Dr, Honolulu, HI 96822

⁵ Center for Astrophysics and Space Sciences, University of California San Diego, MS 0424, La Jolla, CA 92093-0424

*A complete version can be obtained at <http://www.astro.psu.edu/users/misawa/pub/Paper/qalcat.pdf.gz>

ABSTRACT

We have produced a catalog of line identifications and equivalent width measurements for all absorption features in eight ultraviolet echelle quasar spectra. These spectra were selected as having the highest signal-to-noise among the *HST*/STIS spectra obtained with the E230M grating. We identify 56 metal-line systems toward the eight quasars, and present plots of detected transitions, aligned in velocity-space. We found that about 1/4 - 1/3 of the features in the Ly α forest region, redward of the incidence of the Ly β forest, are metal lines. High ionization transitions are common. We see both O VI and C IV in 88 – 90% of the metal-line systems for which the spectra cover the expected wavelength. Si III is seen in 58%, while low ionization absorption in C II, Si II, and/or Al II is detected in 50% of the systems for which they are covered. This catalog will facilitate future studies of the Ly α forest and of metal-line systems of various types.

Key words: intergalactic medium – quasars: absorption lines.

1 INTRODUCTION

The most important chemical transitions for quasar absorption line systems at low redshift (e.g., $z < 1$) still lay in the ultra-violet spectral range. A limited number of the most UV-bright quasars have been observed with the Hubble Space Telescope (*HST*)/ Space Telescope Imaging Spectrograph (STIS), which has provided a detailed view of absorption systems along the lines of sight. These data are available from the Multimission Archive at Space Telescope (MAST). However, in order to compile statistics of absorbers or to study particular systems, it is necessary to identify the spectral features. This can be complicated, particularly in the Ly α forest region, and when the available spectral coverage is limited.

In the course of our studies of the Ly α forest and metal-line systems we have studied in detail eight of the highest quality *HST*/STIS spectra, obtained with the E230M grating. In this paper we present these spectra with a list of 5 σ absorption features and our suggested line identifications. In particular, metal-line system identifications are necessary in order to remove contaminants from the Ly α forest. In a recent paper (Kirkman et al. 2007), we mea-

sured statistics of absorption in the Ly α forest at $0 < z < 1.6$ using 74 low resolution *HST*/FOS quasar spectra. As a check, and particularly to assess our ability to separate metal lines from the forest, we also used the available higher resolution E230M *HST*/STIS spectra. In the present paper, we present the relevant data and line identifications which were used in that paper. We expect that this catalog will facilitate future studies of metal-line absorption systems as well as of the Ly α forest.

Our catalog includes damped Ly α absorbers (DLAs), Lyman limit systems, and Ly α forest clouds. The DLA and Lyman limit systems are expected to have strong Mg II absorption (Rao & Turnshek 2000; Churchill et al. 2000), while the Ly α forest clouds may have weak Mg II and other low ionization transitions detected (such as Si II and C II) (Narayanan et al. 2005). Some Ly α forest clouds have detected C IV and/or O VI, without associated low ionization absorption (Tripp et al. 2000; Savage et al. 2002; Milutinović et al. 2006). The catalog that we will present will allow for future studies of the various types of absorbers.

In § 2 we describe *HST*/STIS quasar spectra and our reduction and continuum fitting procedures. We also outline our line detection and measurement algorithms and line identification strategies. The normalized echelle spectra are presented in § 3, along with a brief description of metal-line systems detected toward each quasar. System plots, showing all detected transitions for each system, are

* Based on observations obtained with the NASA/ESA Hubble Space Telescope, which is operated by the Space Telescope Science Institute (STScI) for the Association of Universities for Research in Astronomy, Inc., under NASA contract NAS5D26555.

also presented there. In § 4 we present a general summary of the systems presented in this catalog.

2 DATA AND METHODS

We selected the eight $z > 1$ quasars observed with the *HST*/STIS E230M grating which had a signal to noise ratio, $S/N > 5$, over a reasonable fraction of the spectrum. These *HST*/STIS E230M spectra have a resolution $R = 30,000$, with two pixels per resolution element. Our sample is biased towards quasars that have Lyman limit systems, since most of the STIS observations were conducted in order to study those particular known systems in detail.

Several settings are possible covering different wavelength ranges. For seven of the eight quasars in our sample, 2280 - 3110 Å is covered. The quasars and the relevant observational details are listed in Table 1. Specifically, this table lists quasar redshifts, wavelength coverage, S/N per pixel at 2350 Å and 2750 Å, primary investigator for the original observation, and proposal ID.

The data were reduced using the STIS pipeline (Brown et al. 2002). They were combined by simple weighting by exposure time (as in Narayanan et al. (2005)), rather than by, e.g., inverse variance methods that are often employed. A bias could be introduced by the latter method, since pixels with smaller counts would be weighted more heavily. This bias is significant only in cases such as these STIS spectra, where individual exposures have very small S/N , and is not typically important for reduction of ground-based high resolution echelle spectra.

Wavelengths were corrected to the heliocentric reference frame. When the same quasar was observed multiple times, there was often a small shift in wavelength between the spectra, due to the intentional shifting of the echelle angle of the instrument. In this case, we chose not to smooth the data by interpolating, but instead chose wavelength bins from one exposure and combined the flux from other exposures into the nearest bin. This results in a slightly decreased effective resolution. Continuum fits used the standard IRAF SFIT task.¹

Features were objectively identified by searching for an unresolved line at each pixel (as employed in Schneider et al. (1993)), and applying a 5σ criterion for detection. However, we found by inspection that some of these formal detections are not likely to be real. In some cases, only 1 pixel had significant absorption, and in other cases it appeared that correlated noise biased the measurement. Features that are broad and shallow can be $> 5\sigma$ and yet look unconvincing because they are sensitive to the continuum level. Such spurious features, estimated to be 10% of the total number of detections, were eliminated from consideration. We define a feature as all the pixels around a 5σ detection that have not recovered to the continuum after smoothing the spectra using an equation on p.56 of Schneider et al. (1993). This definition means that many features are clearly blends of well separated lines, and hence a feature can have more than one identification, each of which may be secure because they refer to different blended lines. Wavelength that we give for a feature is the flux-weighted central value, the mean of the wavelengths where the smoothed flux drops below the continuum, with weighting for the fraction of the photons that are absorbed at each pixel.

We attempted to identify all features in each of the quasar

spectrum, and the transitions that were identified one or more times are listed with their vacuum wavelengths and oscillator strengths in Table 2. For our line identification we used the following procedure:

- (i) Examine the spectrum at the expected positions of possible Galactic lines, and mark all possible detections.
- (ii) Search for the strong resonant doublet transitions: Mg II $\lambda\lambda 2796, 2803$, Si IV $\lambda\lambda 1393, 1402$, C IV $\lambda\lambda 1548, 1551$, N V $\lambda\lambda 1239, 1243$, and O VI $\lambda\lambda 1032, 1038$. In addition to these, we also search for low ionization gas through the combination C II $\lambda 1335$ and Si II $\lambda 1260$, which can be used in place of Mg II $\lambda\lambda 2796, 2803$ when the latter is not covered (Narayanan et al. 2005; Milutinović et al. 2006).
- (iii) Check positions of other transitions that could be detected for systems found through the doublet search, including the Lyman series lines. If a system is ambiguous with the doublet alone, Ly α and other Lyman series lines were used to assess its reality.
- (iv) Having completed these steps, all features that remain without plausible identifications are considered to be Lyman series lines.
- (v) Begin by assuming that the highest order Lyman series line is the correct identification and search for all of the stronger (lower order) Lyman series lines corresponding to the same redshift. If reasonable ratios are found, mark these as possible identifications. Otherwise continue assessing the possible identifications of the feature in question until reaching Ly α .
- (vi) If no identification, including a Ly α identification, is plausible the feature is left unidentified.
- (vii) If more than one identification is reasonable (or if there is likely to be a blend for which more than one system contributes significantly), this is noted.

3 RESULTS

Figure 1a is a sample of a portion of the normalized spectrum of PG0117 + 213, shown in the printed version. We present all other normalized quasar spectra in Figures 1b–8d (see the complete version), which are available electronically at <http://www.blackwellpublishing.com/products/>. Similarly, our listings of line identifications are presented electronically in Table 3, with some sample listings appearing in the printed version. In this table, quasars are ordered by right ascension and 5σ features by increasing wavelength within a given quasar entry. In Table 3 we list, for each 5σ feature that we did not reject as unconvincing, the observed vacuum wavelength (λ_{obs}), the observed frame equivalent width and error (W_{obs} and $\sigma(W_{obs})$), and the significance level (S ; observed equivalent width/ error in equivalent width). It also gives our favored line identification for each feature (transition and redshift) along with notes that indicate alternative and/or additional identifications. If the identification cannot be confirmed with another line, or is uncertain for some other reason, a “?” is listed after the preferred transition ID. We do not give column densities since these are best done on a system by system basis using velocity plots to ensure that the columns for different ions are representative of the same gas.

The following subsections present the eight quasars along with discussion of noteworthy metal-line systems found in their spectra. Figure 9 presents an example “system plot” for the $z = 0.5764$ system toward PG0117 + 213. The transitions detected at 5σ for all of the metal-line systems are plotted in velocity space in the electronic versions of Figures 9–64 (see the complete version). The

¹ IRAF is distributed by the National Optical Astronomy Observatories, which are operated by AURA, Inc., under contract to the National Science Foundation.

quasar emission redshifts, taken from the NASA/IPAC Extragalactic Database, are listed in the heading of each subsection.

3.1 PG0117+213 ($z_{em} = 1.493$)

This quasar was studied as part of the Quasar Absorption Line Key Project, using G270H grating of *HST*/Faint Object Spectrograph (FOS), with resolution of $R=1300$. Jannuzi et al. (1998) found possible metal-line systems at $z = 0.5766, 0.9400, 0.9676, 1.0724, 1.3389, 1.3426$ and 1.3868 . They also found tentative suggestions of metal-line systems at $z = 1.3256$ and 1.4952 . Mg II is detected in a Keck/HIRES spectrum at $z = 0.5764, 0.7290, 1.0480, 1.3250$ and 1.3430 (Churchill & Vogt 2001; Churchill et al. 1999), and these five systems were modeled (including constraints from this STIS coverage) by Masiero et al. (2005).

Jannuzi et al. (1998) observed this quasar with *HST*/STIS to facilitate a statistical study of the Ly α forest. This spectrum covers the Ly α forest over almost all of its wavelength coverage, blueward of 3031 Å. The Ly β line is covered blueward of 2558 Å, Ly γ blueward of 2423 Å, and Ly δ blueward of 2368 Å. There is also limited redshift coverage of higher order Lyman series lines. Along this line of sight are five Mg II absorbers. One of them is a DLA, two are strong Mg II absorbers, and the other two are multiple-cloud, weak Mg II absorbers. Three certain, and two possible O VI systems are also detected. The metal-line systems toward this quasar are plotted in Figures 9–18.

$z = 0.5764$. — The $z = 0.5764$ system is a strong Mg II absorber. Based upon only a low resolution *HST*/FOS spectrum, obtained in spectropolarimetry mode (Koratkar et al. 1998), it is not clear whether this is a DLA or whether it has multiple undamped components (Rao & Turnshek 2000). In the *HST*/STIS spectrum, CIV $\lambda\lambda 1548, 1551$ are detected, but both transitions suffer from blending. The C IV $\lambda 1548$ is blended in its blue component with Ly γ from a system at $z = 1.5088$. An unidentified blend appears on the red wing of C IV $\lambda 1550$ and its blueward component also has a small contribution from Si II $\lambda 1193$ at $z = 1.0480$. Al III $\lambda\lambda 1855, 1863$ is detected, but the blueward member has a blend to its blue, probably with Ly α . Strong Al II $\lambda 1671$ is detected, as is Fe II $\lambda 1608$. The strong feature redward of Al II $\lambda 1671$ is probably Ly α at $z = 1.1671$. In addition to Mg II and Mg I, Ca II and Ti II were detected in the Keck/HIRES spectrum (Masiero et al. 2005).

$z = 0.7290$. — The unusual multiple-cloud, weak Mg II absorber at $z = 0.7290$ is detected only in Al II $\lambda 1671$ and C II $\lambda 1335$ in the *HST*/STIS spectrum. CIV $\lambda\lambda 1548, 1551$ is covered at a high sensitivity, yet it is not detected to a 3σ rest-frame equivalent width limit of 0.01 Å. This makes it “C IV-deficient”, possibly indicative of a low level of star formation so that a corona would be weak or absent in its very red, barred spiral galaxy host (Masiero et al. 2005).

$z = 1.0480$. — The $z = 1.0480$ system was found not to have metal lines detected in the low resolution *HST*/FOS spectrum. The detections of Si II, C II, Si III, Si IV $\lambda\lambda 1393, 1402$ in the *HST*/STIS spectrum are consistent with those limits. Unfortunately, the STIS spectrum does not cover CIV $\lambda\lambda 1548, 1551$, which would provide useful constraints on the system’s physical conditions. Based upon photoionization modeling (Masiero et al. 2005) it would appear that there is a significant blend with Si III $\lambda 1207$, which is most likely Ly α .

$z = 1.3250$. — The $z = 1.3250$ system is just above the borderline to qualify as a strong Mg II absorber. It has six weak

components in Mg II $\lambda\lambda 2796, 2803$ spread over ~ 250 km s $^{-1}$ (Churchill & Vogt 2001). There is a partial Lyman limit system detected in an *HST*/FOS spectrum (Jannuzi et al. 1998). In the *HST*/STIS spectrum Si II and C II are detected from the strongest four of these six components. Si III $\lambda 1207$ is also detected over the full velocity range, but it suffers from a blend with Galactic Mg II $\lambda 2803$ to the blue. There may also be blends redward of this, based upon the photoionization models (Masiero et al. 2005), but we were unable to provide identifications besides possible Ly α . Unfortunately, CIV $\lambda\lambda 1548, 1551$, which was detected in the *HST*/FOS spectrum (Jannuzi et al. 1998), is not covered in the STIS spectrum. There is a possible weak detection of N V $\lambda 1239$ but it cannot be confirmed using N V $\lambda 1243$ because it is in a noisy part of the spectrum. A strong O VI $\lambda\lambda 1032, 1038$ is detected, but O VI $\lambda 1032$ is blended to the red with Ly β from the system at $z = 1.3390$, and to the blue with possible Ly α . Also, O VI $\lambda 1038$ must have a blend, at least on the red wing of its strong component, since that profile is too strong relative to O VI $\lambda 1032$ at that velocity. This blend could be O VI $\lambda 1032$ from the $z = 1.3390$ system. If so, these systems would be “line-locked”.

$z = 1.3390$. — We find the evidence for metal lines in the $z = 1.3390$ system to be inconclusive. Ly α is not detected in the redward portion range of the possible C III $\lambda 977$ feature, so not all of that absorption can be C III at this redshift. Two components of Si III $\lambda 1207$ are possible, but they do not align perfectly with the minima of the C III profile and cannot be confirmed in any other way. Also, O VI $\lambda\lambda 1032, 1038$ may be detected. The alignment is reasonably good, though the feature redward of the O VI $\lambda 1032$ component is likely to be O VI $\lambda 1038$ from the system at $z = 1.3250$.

$z = 1.3430$. — The $z = 1.3430$ system is also just at the border between strong and multiple-cloud weak Mg II absorption. Like the $z = 1.3250$ system, it has a partial Lyman limit break in the *HST*/FOS spectrum (Jannuzi et al. 1998). Ly α and Ly β are detected in the *HST*/STIS spectrum along with C II, Si II, N II, C III. There is a feature at the expected position of N III $\lambda 998$, which appears to be too strong relative to the other transitions in this system (Masiero et al. 2005). We believe this feature could be Ly α at $z = 0.9076$. C IV is not covered in the STIS spectrum, but strong C IV absorption is detected in the FOS spectrum. N V $\lambda\lambda 1239, 1243$ appears to be detected, but the N V $\lambda 1239$ transition is blended, probably with Ly α at $z = 1.3866$.

$z = 1.4242$. — There is an O VI system, with detected Ly α , Ly β , and Ly γ at $z = 1.4242$.

$z = 1.4463$. — Another weak, broad O VI doublet at $z = 1.4463$ is also detected in C III and Si III, as well as in Ly α . The feature in the Si III $\lambda 1207$ panel, at ~ 40 km s $^{-1}$, is at least partially Si II $\lambda 1260$ at $z = 1.3430$ (as is the stronger feature to its red).

$z = 1.4478$. — At $z = 1.4478$ the Lyman series is detected down to Ly ϵ , which is the last member covered in the *HST*/STIS spectrum. There is a possible O VI doublet at this redshift, but the feature at the position of O VI $\lambda 1032$ transition does not match the profile of that at the position of O VI $\lambda 1038$.

$z = 1.5088$. — The O VI system at $z = 1.5088$ is another example of associated O VI absorption that appears slightly redward of the quasar emission redshift. It is detected in Ly α and Ly β . The Ly β shows the same components as O VI, but clearly has a blend to the red, probably with Ly α . Ly γ is heavily blended with C IV $\lambda 1548$ from the $z = 0.5764$ system. C III $\lambda 977$ is also detected in three components, though the blueward one is affected by a data defect.

3.2 HE0515-4414 ($z_{em} = 1.713$)

This quasar was observed with *HST*/STIS by Reimers et al. (2003) in order to study a sub-DLA at $z = 1.15$, for which they also have optical coverage. Their study of this system, particularly focused on molecular hydrogen, is published as Reimers et al. (2003). In addition, Reimers et al. (2003) and Levshakov et al. (2003) report on six O VI systems along the line of sight (at $z = 1.385, 1.416, 1.602, 1.674$ and 1.697), based upon the *HST*/STIS spectrum in conjunction with VLT/UVES data. Ly α is covered over the entire *HST*/STIS spectrum, Ly β up to 2784 \AA , and Ly γ is covered up to 2651 \AA . There is more limited coverage of all other Lyman series transitions down to the Lyman limit of the quasar.

The *HST*/STIS spectrum is dominated by the sub-DLA at $z = 1.15$ and its many detected metal and molecular hydrogen transitions. In addition, there is one C IV system, four definite O VI systems, and three possible O VI systems. A couple of these O VI systems are associated. System plots for this quasar are given in Figures 19–27.

$z = 0.9406$. — A two component C IV doublet is detected at $z = 0.9406$, which also has Ly α and Si III detected. Si IV is also probably detected in the redward component, but this can't be confirmed because Si IV $\lambda 1394$ is blended with an unknown line, probably Ly α .

$z = 1.1508$. — The sub-DLA at $z = 1.1508$ is a very complex system, spanning 800 km s^{-1} for absorption in many low ionization transitions. It has many molecular hydrogen lines detected. Our identifications for the molecules follow exactly those of Reimers et al. (2003). The saturated region of the sub-DLA profile spans $\sim 1100 \text{ km s}^{-1}$. A separate component at $\sim -900 \text{ km s}^{-1}$ is likely also to be Ly α , but with no associated metals in the *HST*/STIS spectrum. Many neutral species of C I and N I are detected in a single, narrow component at $\sim 0 \text{ km s}^{-1}$, presumably associated with the bulk of the H I. Features at other velocities seen in the neutral transitions panels in Figure 20 are not related to this system (see line identifications in Table 3). O I $\lambda 1302$ is blended with Ly α at $z = 1.3039$, and cannot be measured, and no other strong O I transitions are covered. Many singly ionized transitions are detected for the system, both in the 0 km s^{-1} component and at many other velocities to the blue. These match the Mg II and Fe II from the VLT/UVES spectrum (Levshakov et al. 2003). Strong Si III absorption is detected in many components, spanning the full velocity range. Si IV $\lambda\lambda 1393, 1402$ is detected as well, but there appears to be significant blending with Si IV $\lambda 1394$, because Si IV $\lambda 1403$ is much weaker at some velocities. CIV $\lambda\lambda 1548, 1551$ is also detected in the VLT/UVES spectrum. NV $\lambda\lambda 1239, 1243$ is covered, but not detected, and O VI $\lambda\lambda 1032, 1038$ is not covered.

$z = 1.3849$. — An O VI doublet detected in the *HST*/STIS spectrum at $z = 1.3849$ has its $\lambda 1038$ member blended to the blue with Ly β at 1.4124 . CIV $\lambda\lambda 1548, 1551$ is detected at the same redshift in the VLT/UVES spectrum (Levshakov et al. 2003). The corresponding, relatively weak (unsaturated) Ly α line lies blueward of a larger saturated Ly α feature. C III may also be detected.

$z = 1.4163$. — There is a possible O VI system at $z = 1.4163$, as reported by Levshakov et al. (2003), however neither member of the O VI doublet aligns with the Ly α and Ly β , which are also detected in the STIS spectrum. There could be C III associated with this system, but it is badly blended with a probable Ly α line, thus its alignment cannot be verified. Therefore, there is not convincing evidence for detected metals in this system.

$z = 1.6020$. — The O VI system at $z = 1.6020$ is well aligned and is detected in Ly β and Ly γ in the *HST*/STIS spectrum.

Ly α , and possibly C IV, is detected in the VLT/UVES spectrum (Levshakov et al. 2003).

$z = 1.6668$. — There is a possible O VI system at $z = 1.6668$, though its identity is somewhat uncertain. O VI $\lambda 1038$ is blended with a possible Ly α line, such that the profiles of the doublet members cannot be compared. Ly β is not detected at the position, however Ly α is detected, with about the same profile shape and equivalent width as the O VI. Thus, this could be a fairly typical associated O VI absorber.

$z = 1.6736$. — There is an O VI system at $z = 1.6736$ detected in the *HST*/STIS spectrum. O VI $\lambda 1038$ is blended to the red with a possible Ly α line. Ly β is detected, as are higher order Lyman series lines, but the latter are blended with other transitions (see Table 3). CIV $\lambda\lambda 1548, 1551$ and Ly α are detected in the VLT/UVES spectrum (Levshakov et al. 2003).

$z = 1.6971$. — The associated O VI absorber at $z = 1.6971$ also has C III $\lambda 977$ and probably S VI $\lambda 933$ detected. Levshakov et al. (2003) also detected Ly α , Si IV $\lambda\lambda 1393, 1402$, CIV $\lambda\lambda 1548, 1551$, and NV $\lambda\lambda 1239, 1243$ in their VLT/UVES spectrum. The Ly α profile is not black, again a signature of associated O VI absorbers.

$z = 1.7358$. — A possible O VI system at $z = 1.7358$ cannot be confirmed by other features in the *HST*/STIS spectrum. Although Ly β is covered, it is blended with Galactic Mg II $\lambda 2803$. If real, this system would be significantly redshifted relative to the emission redshift of the quasar.

3.3 PG1206+459 ($z_{em} = 1.16254$)

This quasar was observed by *HST*/FOS as part of the Quasar Absorption Line Key Project, but they had difficulty in identifying many of the lines due to uncertain continuum fitting (Jannuzi et al. 1998). They found evidence for an extensive metal-line system separated into subsystems at $z = 0.9254, 0.9277$ and 0.9342 , even at low resolution. Churchill et al. (1999) modeled this system based on the *HST*/FOS data, along with Keck/HIRES data (Churchill & Vogt 2001). Ding et al. (2003) refined these models once the *HST*/STIS spectra were available.

Churchill et al. (1999) observed this quasar with *HST*/STIS to facilitate a detailed study of the systems at $z \sim 0.927$. The *HST*/STIS spectrum covers the Ly α forest blueward of 2628 \AA , but does not cover any higher order Lyman series lines. There are only three metal-line systems found in the *HST*/STIS spectrum: the extensive metal-line system at $z \sim 0.927$ mentioned above, a C IV system, and an associated N V system. Figure 28–32 presents system plots for these metal-line systems, detected toward PG1206 + 459.

$z = 0.7338$. — There is a weak C IV doublet at $z = 0.7338$. The C IV $\lambda 1548$ is blended with Si IV $\lambda 1394$ from the subsystem at $z = 0.9254$, and also to the red with an unknown blend, probably Ly α . The large feature blueward of the C IV $\lambda 1551$ transition is Si IV $\lambda 1394$ at $z = 0.9276$. Mg II is not detected in the Keck/HIRES spectrum, nor any other low ionization transitions in the *HST*/STIS spectrum. However, the system is confirmed by Ly α in the *HST*/FOS spectrum.

$z = 0.9254$. — The complex metal-line system at $z = 0.9277$ is spread over more than 1000 km s^{-1} . Ding et al. (2003) separated it into three systems at $z = 0.9254$ (System A), $z = 0.9277$ (System B), and $z = 0.9342$ (System C). They suggest that these systems are produced by three different galaxies in a group. System A, at $z = 0.9254$, has detected C II, Si III, Si IV $\lambda\lambda 1393, 1402$, CIV $\lambda\lambda 1548, 1551$, and NV $\lambda\lambda 1239, 1243$ in the *HST*/STIS spec-

trum. Many other transitions, including O VI $\lambda\lambda 1032, 1038$ and Lyman series lines, were detected in the *HST*/FOS spectrum. Si IV $\lambda 1394$ is blended with C IV $\lambda 1548$ from the $z = 0.7338$ C IV system. Ly α is saturated and covers the entire velocity range between this system and System B.

$z = 0.9276$. — System B, at $z = 0.9276$, produces a partial Lyman limit break in the *HST*/FOS spectrum. It is detected in several transitions of Si II, C II, Si III, Si IV $\lambda\lambda 1393, 1402$, C IV $\lambda\lambda 1548, 1551$, and N V $\lambda\lambda 1239, 1243$. Galactic Fe II $\lambda 2344$ is blended with the red wing of the Ly α profile. C II $\lambda 1335$ is blended to the red with an unidentified line, probably Ly α . The feature redward of Si IV $\lambda 1394$ is C IV $\lambda 1551$ from the $z = 0.7338$ system. C IV is self-blended, with the C IV $\lambda 1551$ from System A superimposed on the C IV $\lambda 1548$ from System B.

$z = 0.9343$. — System C, at $z = 0.9343$ is unusual in its high velocity relative to the main system, System B. For this system, which would be considered a single-cloud, weak Mg II absorber if isolated from the other systems, is detected in Ly α , Si II, C II, Si III, Si IV $\lambda\lambda 1393, 1402$, and C IV $\lambda\lambda 1548, 1551$. N V $\lambda 1239$ is blended with N V $\lambda 1243$ from System B, but N V $\lambda 1243$ is not detected in a clean part of the spectrum. Again, O VI and various other transitions are detected in the *HST*/FOS spectrum.

$z = 1.0281$. — The N V system at $z = 1.0281$ is almost certainly intrinsic judging by its broad profile and the “non-black” Ly α line, evidence for partial covering. No other metals are detected besides the N V.

3.4 PG1241+176 ($z_{em} = 1.273$)

This was also a quasar studied for the Quasar Absorption Line Key Project (Jannuzi et al. 1998), and a Keck/HIRES spectrum was obtained by Churchill & Vogt (2001). Particular Mg II systems, with optical and UV coverage, were studied in Churchill et al. (2000). The $z = 0.5505, 0.5584$ and 0.8954 systems were modeled in detail by Ding et al. (2005).

This quasar was observed with *HST*/STIS by Churchill et al. in order to provide constraints on the physical conditions in Mg II absorbers. Ly α forest lines appear in *HST*/STIS spectrum quasar spectrum blueward of 2763 \AA , and the Ly β forest is covered blueward of 2332 \AA . We find evidence for six metal-line systems: one strong Mg II absorber, two weak Mg II absorbers, one weak C IV, and two associated O VI absorbers. The system plots for these metal-line systems are shown in Figures 33–38.

$z = 0.5507$. — Jannuzi et al. (1998) found a metal-line system at $z = 0.5507$ with strong C IV detected. This system corresponds to a strong Mg II absorber detected in a Keck/HIRES spectrum (Churchill & Vogt 2001), which also has detected Ca II, Fe II, and Mg I. In the *HST*/STIS spectrum, we also find Fe II $\lambda 1608$, Al II $\lambda 1671$, and C IV $\lambda\lambda 1548, 1551$. There is a 3σ detection of Al II $\lambda 1671$ at $v \sim 150 \text{ km s}^{-1}$, which coincides with a satellite component of Mg II $\lambda\lambda 2796, 2803$ in the Keck/HIRES spectrum (Ding et al. 2005).

$z = 0.5584$. — For the multiple-cloud, weak Mg II absorber at $z = 0.5584$, C IV $\lambda\lambda 1548, 1551$ was detected in the *HST*/STIS spectrum, but no low ionization transitions were detected, though Al II $\lambda 1671$, Al III $\lambda\lambda 1855, 1863$, and Si II $\lambda 1527$ were covered.

$z = 0.7577$. — A possible weak C IV doublet at $z = 0.7577$ cannot be confirmed, since Ly α is not covered in the *HST*/STIS or in the previous *HST*/FOS spectrum.

$z = 0.8954$. — The single-cloud, weak Mg II absorber at $z = 0.8954$ has detected Ly α , Si III $\lambda 1207$, Si IV $\lambda 1394$, and

C IV $\lambda\lambda 1548, 1551$. The Si IV $\lambda 1403$ is affected by a blend. Although there is a detection at the position of Si II $\lambda 1260$, Ding et al. (2005) note that this may be a blend, since it is difficult to explain the strength of this feature in comparison to the weaker Mg II $\lambda\lambda 2796, 2803$ lines.

$z = 1.2152$. — The O VI system, at $z = 1.2152$, found by Jannuzi et al. (1998) is confirmed here, showing O VI $\lambda\lambda 1032, 1038$ and Ly α in the *HST*/STIS spectrum. Although a feature is detected at the position of N V $\lambda 1239$, also noted by Jannuzi et al. (1998), this is inconsistent with the lack of detection of N V $\lambda 1243$, and so cannot be confirmed.

$z = 1.2717$. — Jannuzi et al. (1998) found a strong associated O VI absorber at $z = 1.2717$ in their *HST*/FOS spectrum, for which Ly α and Ly β were also detected. In the higher resolution *HST*/STIS spectrum, we confirm these detections, but do not find any other associated absorption. The relatively weak Ly α , as compared to O VI $\lambda\lambda 1032, 1038$ is characteristic of a class of associated O VI absorbers (Ganguly et al. 2007, in preparation).

3.5 PG 1248+401 ($z_{em} = 1.030$)

This quasar was studied by the *HST* Quasar Absorption Line Key Project using G190H and G270H spectra obtained with FOS (Jannuzi et al. 1998), who found metal-line systems at $z = 0.3946, 0.7660, 0.7732$ and 0.8553 . The latter two systems correspond to strong Mg II absorbers, modeled by Ding et al. (2005) based on Keck/HIRES data (Churchill & Vogt 2001) and the *HST*/STIS spectrum presented here. Another system, at $z = 0.7011$, with only C IV $\lambda\lambda 1548, 1551$ and Ly α detected, was discussed in Milutinović et al. (2006).

Churchill et al. (1999) obtained a spectrum of this quasar with *HST*/STIS in order to provide constraints on the physical conditions in the two strong Mg II absorbers along the line of sight. In the *HST*/STIS spectrum, the Ly α forest is only covered up to a wavelength of 2468 \AA , and higher order Lyman series lines are not covered. We find evidence for two strong Mg II and two weak C IV systems in the *HST*/STIS spectra. These systems are shown in Figures 39–45.

$z = 0.3946$. — Al II $\lambda 1671$ and Al III $\lambda 1855$ are the only prominent transitions from the possible $z = 0.3946$ system that are covered in the *HST*/STIS spectrum. Although there is a detection at the position of Al II $\lambda 1671$, the lack of detected Al III $\lambda\lambda 1855, 1863$ and the lack of detection of C IV $\lambda\lambda 1548, 1551$ in the FOS spectrum leads us to question the reality of this system. Thus we prefer an identification of the feature at 2330.09 \AA as Ly α .

$z = 0.5648$. — A C IV doublet is found at $z = 0.5648$ in the *HST*/STIS spectrum. It is confirmed by a Ly α detection in the G190H *HST*/FOS spectrum (Jannuzi et al. 1998). The weak feature at the expected position of Si II $\lambda 1527$ is unlikely to be Si II because of the absence of the stronger Si II $\lambda 1260$ transition in the FOS spectrum.

$z = 0.6174$. — There is a very weak possible C IV doublet at $z = 0.6174$ in the *HST*/STIS spectrum, however the alignment is not perfect. Also, there is no Ly α detected in the FOS spectrum to a rest frame equivalent width limit of 0.11 \AA .

$z = 0.7011$. — The C IV absorption system at $z = 0.7011$ is confirmed by a Ly α detection in the FOS spectrum, but there are no additional detections in the *HST*/STIS spectrum.

$z = 0.7728$. — The strong Mg II system at $z = 0.7728$ has detected Al II $\lambda 1671$, Si II $\lambda 1304$ and Si II $\lambda 1527$, C II $\lambda 1335$, Si IV $\lambda\lambda 1393, 1402$, and C IV $\lambda\lambda 1548, 1551$ in the STIS E230M

spectrum. O I $\lambda 1302$ may be detected in the strongest low ionization component, but the spectrum is very noisy in that region.

$z = 0.7760$. — We cannot confirm a system at $z = 0.7760$, which was suggested by Jannuzi et al. (1998), however we note that we also do not detect C IV $\lambda\lambda 1548, 1551$ to a 3σ rest frame equivalent width limit of 0.02 \AA . It is still possible that this system exists, but is collisionally ionized, as proposed by Jannuzi et al. (1998).

$z = 0.8545$. — The strong Mg II system at $z = 0.8545$ has detected Si II $\lambda 1260$, C II $\lambda 1335$, Si IV $\lambda\lambda 1393, 1402$, C IV $\lambda\lambda 1548, 1551$, and N V $\lambda\lambda 1239, 1243$. Kinematically, this system is interesting, with satellite components in low ionization gas (offset $\sim 300 \text{ km s}^{-1}$ from the main absorption) having corresponding, broader C IV absorption.

3.6 CSO 873 ($z_{em} = 1.022$)

This quasar was previously studied through G190H and G270H *HST*/FOS spectra (Bahcall et al. 1996), but only three metal-line systems were indicated, at $z = 0.2891, 0.6606$ and 1.0022 . The $z = 0.6606$ coincides with a strong Mg II absorber (Churchill & Vogt 2001), and it was modeled by Ding et al. (2005).

The *HST*/STIS spectrum was obtained in a program (P.I. Churchill) to facilitate a study of the $z = 0.6606$ Mg II absorber. This spectrum covers the Ly α forest up to a wavelength of 2458 \AA , and does not cover any Ly β lines.

$z = 0.6611$. — Besides Galactic absorption, in the *HST*/STIS E230M spectrum, we detect metal-line absorption from only the system at $z = 0.6611$, which corresponds to a full Lyman limit break seen in a *HST*/FOS G160L spectrum (Bahcall et al. 1993, 1996). A system plot is shown in Figure 46. From this system we find Al II $\lambda 1671$, Si II $\lambda 1527$, and C IV $\lambda\lambda 1548, 1551$. Si IV is not detected. In fact, the C IV absorption at the velocity of the low ionization absorption is relatively weak, and this system classifies as “C IV-deficient” (Ding et al. 2005). The strongest C IV absorption is $\sim 200 \text{ km s}^{-1}$ redward of the strongest low ionization component. Jannuzi et al. (1998) note a complex of Ly α lines ranging from $z = 0.6692$ to 0.6771 . They found no metals associated with this complex in the low resolution *HST*/FOS spectrum. We note that with the STIS data, it is possible to set a stronger limit, with a rest frame 3σ equivalent width limit $W_r(1548) < 0.02A$.

3.7 PG1634 + 706 ($z_{em} = 1.334$)

This was one of the *HST* QSO Absorption Line Key Project quasars, and its *HST*/FOS G270M spectrum was presented in Bahcall et al. (1996). In that spectrum, three extensive metal-line systems are present at $z = 0.9060, 0.9908$ and 1.0417 . Also, there are possible C IV doublets at $z = 0.5582, 0.6540, 0.6790$ and 0.7796 , and a possible O VI doublet at $z = 1.3413$. In a Keck/HIRES optical spectrum, strong Mg II absorption is detected from the $z = 0.9908$ system, and weak Mg II absorption from the $z = 0.6540, 0.9060$ and 1.0417 systems (Churchill & Vogt 2001; Churchill et al. 1999; Charlton et al. 2003). Weak Mg II is also detected at $z = 0.8181$ in the optical spectrum (Churchill et al. 1999). The three single-cloud, weak Mg II absorbers at $z = 0.8181, 0.9056$ and 0.6534 were modeled by Charlton et al. (2003), the multiple-cloud, weak Mg II absorber at $z = 1.0414$ by Zonak et al. (2004), and the strong Mg II absorber at $z = 0.9902$ by Ding et al. (2003).

Two programs contribute different wavelength coverage of this quasar with *HST*/STIS. Buries (1997, HST Proposal ID #7292)

observed the quasar in order to measure the primordial D/H ratio. Jannuzi et al. (1998) provided redward coverage in order to conduct a detailed study of the Ly α forest. In the *HST*/STIS spectra, Ly α is covered up to 2837 \AA , Ly β up to 2395 \AA , and Ly γ in the small region up to 2268 \AA . There is detected absorption from the strong Mg II absorber, and from the four weak Mg II absorbers mentioned above. There are also several possible C IV systems and a possible O VI system, as well as an interesting “C III/Si III-only” system. There is a possible intrinsic N V system and an associated O VI system observed toward this quasar as well. We report on these systems here, and shown system plots in Figures 47–56.

$z = 0.2854$. — We can only tentatively claim a C IV doublet at $z = 0.2854$. The C IV $\lambda 1548$ and C IV $\lambda 1551$ profiles match reasonably well, but C IV $\lambda 1551$ may be a bit too strong at some velocities, and there is no coverage of transitions that could confirm this identification. This could relate to a blend with the C III $\lambda 977$ from the $z = 1.0415$ system (see below).

$z = 0.6513$. — There is also a probable, narrow C IV doublet at $z = 0.6513$. The C IV $\lambda 1550$ transition is blended with C IV $\lambda 1548$ from the $z = 0.6535$ system. If this is real, it is unusual in the weakness of Ly α relative to C IV. A weak, narrow N V doublet may also be detected.

$z = 0.6535$. — The *HST*/STIS spectrum shows weak absorption in several low and intermediate transitions related to the $z = 0.6535$ single-cloud, weak Mg II absorber. The C IV has two components redward of the dominant low ionization absorption, and Si IV is weaker but has similar kinematics.

$z = 0.8182$. — The single-cloud, weak Mg II absorber at $z = 0.8182$ has detected Si II, C II, Si IV, and C IV absorption, all centered at the same velocity as the Mg II. Si III $\lambda 1206$ is blended with Ly β from a system at $z = 1.1382$, and is apparent as a small depression in the red wing of that feature.

$z = 0.9056$. — For another single-cloud, weak Mg II absorber at $z = 0.9056$, Ly α , Ly β , C II, Si II, Si IV, C IV, N V, and O VI are detected in the *HST*/STIS spectrum. The coverage of N V and O VI is unusual for single-cloud, weak Mg II absorbers and is important for considerations of the phase structure of these objects.

$z = 0.9645$. — There is an interesting system detected in the *HST*/STIS spectrum at $z = 0.9645$. Most of the common metal transitions have good coverage, but only C III and Si III are detected. Ly α and Ly β confirm the reality of this system.

$z = 0.9904$. — The C IV-deficient, strong Mg II absorber at $z = 0.9904$ has detections in the *HST*/STIS spectrum of the first four Lyman series lines, O I, and a variety of singly to triply ionized transitions, including relatively weak C IV absorption. N V and O VI are covered, but not detected. The Ly δ line is detected, but suffers from a blend to the blue with H I $\lambda 926$ from the system at $z = 1.0415$. This system is of interest because the higher ionization transitions appear redward of the lower ionization transitions, indicating a density gradient across the system (Ding et al. 2005).

$z = 1.0415$. — The $z = 1.0415$ multiple-cloud, weak Mg II system has a partial Lyman limit break detected in a *HST*/STIS G230M spectrum. The higher order Lyman series lines are detected down to the break in the *HST*/STIS E230M spectrum, though past H I $\lambda 919$ they suffer badly from blending with the Lyman series lines from the $z = 0.9904$ system. Metal lines are detected in Si II, C II, Si III, Si IV, and O VI from each of two subsystems. The low ionization transitions are centered at different velocities than the high ionization transitions. C III $\lambda 977$ is also detected, but may be blended with the possible C IV doublet at $z = 0.2854$. C IV is detected in a

low resolution *HST*/FOS spectrum, but is redward of the *HST*/STIS coverage.

$z = 1.1408$. — There is a possible O VI absorber at $z = 1.1408$, however its O VI $\lambda 1032$ transition is too strong relative to the O VI $\lambda 1038$ transition. Although Ly α , Ly β , and Ly γ are detected at this velocity, their relative strengths are also inconsistent, perhaps due to unknown blends.

$z = 1.3413$. — An O VI doublet is detected from a system at $z = 1.3413$, which is slightly redward of z_{em} . It is confirmed by a very weak Ly α detection, but Ly β is badly blended and provides no additional constraint. This is another example of an associated O VI system (e.g. Ganguly et al. (2007, in preparation)).

3.8 PG1718 + 481 ($z_{em} = 1.084$)

The E230M observation of this quasar with *HST*/STIS was proposed by Burles et al. (1997, HST Proposal ID #7292) to facilitate a study of the deuterium to hydrogen ratio in a system at $z = 0.701$ (Kirkman et al. 2001). An *HST*/STIS G230M spectrum was also obtained, covering the Lyman series for this system (Kirkman et al. 2001). Earlier, this quasar was observed as part of the HST Quasar Absorption Line Key Project. Jannuzi et al. (1998) found metal-line systems at $z = 0.8929$, 1.0323 and 1.0872.

In the *HST*/STIS spectrum, Ly α is covered up to 2535 Å, Ly β up to 2138 Å, and Ly γ up to 2036 Å. All Lyman series lines are covered below 1902 Å. In addition to the $z = 0.701$ system, for which this observation was obtained, we find evidence for four definite and two possible O VI absorbers. These systems are all shown in Figures 57–64.

$z = 0.7011$. — The $z = 0.7011$ Lyman limit system has Ly α and Si III detected in the *HST*/STIS spectrum. Weak C II $\lambda 1335$ also appear to be detected, consistent with the weak Mg II absorption that Kirkman et al. (2001) found in a HIRES/Keck spectrum. C IV $\lambda\lambda 1548, 1551$ and Si IV $\lambda\lambda 1393, 1402$ are covered, but not detected.

$z = 0.8928$. — An O VI absorber is found at $z = 0.8928$ in the STIS spectrum, accompanied by detections of Si III, Ly α , and Ly β . Jannuzi et al. (1998) also found C III in a low resolution *HST*/FOS spectrum.

$z = 1.0065$. — Another O VI system is detected at $z = 1.0065$ in the *HST*/STIS spectrum. Ly α and Ly β are also detected, confirming this O VI doublet.

$z = 1.0318$. — A stronger O VI absorber is detected at $z = 1.0318$, corresponding to the system found by Jannuzi et al. (1998). In the *HST*/STIS spectrum the first five Lyman series lines are detected, along with C III, N V $\lambda\lambda 1239, 1243$, and O VI $\lambda\lambda 1032, 1038$.

$z = 1.0507$. — There is a feature detected (just above 5σ) at the position of O VI $\lambda 1032$ for a system at $z = 1.0507$ with detected Ly α and Ly β absorption. The O VI $\lambda 1038$ is not detected, even at 2σ , so it is uncertain whether there are detected metals for this system.

$z = 1.0548$. — The $z = 1.0548$ system, with Ly α , Ly β , Ly γ , and Ly δ detected in the *HST*/STIS spectrum, appears to be an O VI absorber, with weak C III absorption. The O VI doublet cannot be confirmed because the O VI $\lambda 1032$ member is blended with Ly β at $z = 1.0674$.

$z = 1.0867$. — There is an associated system with $z = 1.0867$, detected in Ly α , Ly β , and Ly γ . The Ly α profile has a black, saturated region at this redshift. The $z = 1.0867$ component has detections in C III and Si III.

$z = 1.0874$. — There is also a non-black component at $z = 1.0874$. This system detected O VI $\lambda\lambda 1032, 1038$, and resembles many other associated O VI systems.

4 SUMMARY OF SYSTEMS

This paper presents a catalog that is useful for investigations of metal-line systems and the Ly α forest in eight of the highest S/N-ratio E230M spectra from the *HST*/STIS archive. We have identified a total of 56 metal-line systems (with at least one metal line detected) toward the eight quasars listed in Table 1, as presented in Figures 9–64. For key transitions, Table 4 tabulates in how many of the 56 systems a given transition was covered and in how many it was detected. We must caution that clearly these numbers apply only to this particular dataset and are highly dependent on the detection limits of the spectra, to the exact wavelength coverage, and to biases toward certain kinds of quasars for the sample. In this sample of eight quasars, there may be a preference toward strong low ionization absorbers, since many of them were chosen for a program to study the C IV associated with Mg II absorption (see Table 1).

Nonetheless, it is useful to note from Table 4 that for about half of the 56 systems we have coverage of the C IV and O VI doublets, and that in those cases these high ionization transitions were detected $\sim 90\%$ of the time. Intermediate ionization transitions such as C III $\lambda 977$ and Si III $\lambda 1207$ were also covered about half the time, and were detected in 50%/58% of the sight lines, respectively. C II $\lambda 1335$ is also covered for about half of the systems, and was detected 56% of the time, while Si II $\lambda 1260$ was only detected in 36% of the sightlines for which it was covered. We conclude that almost all $1 < z < 1.7$ metal-line systems have high ionization absorption detected, but that only half have detected low ionization absorption. These numbers are consistent with the findings of Milutinović et al. (2006), that half of all C IV absorbers at low redshift have detected low ionization absorption (sometimes weak), and that the other half do not. This is not surprising since the samples used for these studies have considerable overlap.

Studies of the statistics of the Ly α forest can be significantly affected by metal lines in the forest. With our catalog we are able to give an indication of the level of contamination by metal lines in the $1.0 < z < 1.7$ forest. Specifically, we scanned the wavelength regions of our catalog that are in the Ly α forest of the quasar, but are redward of the Ly β forest. Table 1 lists how many Ly α lines and how many metal lines were detected in this region for each quasar. It also shows that 9–10 of the features detected in the E230M quasar spectra are actually Galactic absorption. We conclude that of the $1.0 < z < 1.7$ Ly α forest lines detected toward each of the quasars (redward of the Ly β forest), 20–33% of the lines in the Ly α forest are actually metal lines. This "contamination" is significant enough that it is important to remove it before computing the statistics of the Ly α lines, and is clearly itself a complicated function of redshift.

ACKNOWLEDGMENTS

We acknowledge support from NASA under grant NAG5-6399 NNG04GE73G and by the National Science Foundation under grant AST 04-07138. J. R. M. and R. S. L. were partially funded by the NSF Research Experience for Undergraduates (REU) program. DT and DK were supported in part by STScI grants HST-AR-10688

and HST-AR-10288. SB was supported by the NSF/REU program in the summer of 2005.

REFERENCES

- Bahcall J. N., et al., 1996, *ApJ*, 457, 19
 Bahcall J. N., et al., 1993, *ApJS*, 87, 1
 Brown, T., et al. 2002, *HST STIS Data Handbook*, version 4.0, ed. B. Mobasher (Baltimore; STScI)
 Charlton, J. C., Ding, J., Zonak, S. G., Churchill, C. W., Bond, N. A., & Rigby, J. R. 2003, *ApJ*, 589, 311
 Churchill, C. W., Mellon, R. R., Charlton, J. C., Jannuzi, B. T., Kirhakos, S., Steidel, C. C., & Schneider, D. P. 2000, *ApJS*, 130, 91
 Churchill, C. W., Rigby, J. R., Charlton, J. C., & Vogt, S. S. 1999, *ApJS*, 120, 51
 Churchill, C. W., & Vogt, S. S. 2001, *AJ*, 122, 679
 Ding, J., Charlton, J. C., & Churchill, C. W. 2005, *ApJ*, 621, 615
 Ding, J., Charlton, J. C., Churchill, C. W., & Palma, C. 2003a, *ApJ*, 590, 746
 Ding J., Charlton J. C., Bond N. A., Zonak S. G., Churchill C. W., 2003b, *ApJ*, 587, 551
 Ganguly R. et al., 2007, in preparation
 Jannuzi B. T., et al., 1998, *ApJS*, 118, 1
 Kirkman, D., Tytler, D., Lubin, D., & Charlton, J. 2007, *MNRAS*, 376, 1227
 Kirkman, D., et al. 2001, *ApJ*, 559, 23
 Koratkar A., Antonucci R., Goodrich R., Storrs A., 1998, *ApJ*, 503, 599
 Levshakov S. A., Agafonova I. I., Reimers D., Baade R., 2003, *A&A*, 404, 449
 Masiero, J. R., Charlton, J. C., Ding, J., & Churchill, C. W. 2005, *ApJ*, 623, 57
 Milutinović N., Rigby J. R., Masiero J. R., Lynch R. S., Palma C., Charlton J. C., 2006, *ApJ*, 641, 190
 Narayanan, A., Charlton, J. C., Masiero, J. R., & Lynch, R., 2005, *ApJ*, 632, 92
 Rao, S. M., & Turnshek, D. A., 2000, *ApJS*, 130, 1
 Reimers D., Baade R., Quast R., Levshakov S. A., 2003, *A&A*, 410, 785
 Savage, B. D., Sembach, K. R., Tripp, T. M., & Richter, P., 2002, *ApJ*, 564, 631
 Schneider, D. P., et al. 1993, *ApJS*, 87, 45
 Tripp, T. M., Savage, B. D., & Jenkins, E. B. 2000, *ApJ*, 534, L1
 Verner, D. A., Verner, E. M., & Ferland, G. J. 1996, *ADNDT*, 64, 1
 Zonak, S. G., Charlton, J. C., Ding, J. & Churchill, C. W. 2004, *ApJ*, 606, 196

Table 1. *HST*/STIS E230M Quasar Observations

QSO ID	z_{em}	S/N^a		PI	Proposal ID	λ_{lo} (Å)	λ_{up} (Å)	N_{tot}^b	N_{metal}^c	N_{Gal}^d
		2382 Å	2796 Å							
PG 0117+210	1.491	8.5	14.2	Jannuzi	8673	2278.7	3117.0	104	31	10
HE 0515-4414	1.713	8.1	22.0	Reimers	8288	2274.8	3118.9	63	13	9
PG 1206+459	1.160	8.4	15.4	Churchill	8672	2277.1	3116.4	85	33	9
PG 1241+176	1.273	5.2	20.0	Churchill	8672	2276.9	3066.0	62	20	10
PG 1248+401	1.030	8.1	9.6	Churchill	8672	2276.7	3107.7	41	14	10
CSO 873 ^e	1.022	8.0	10.4	Churchill	8672	2278.4	3119.2	26	3	8
PG 1634+706	1.334	19.8	28.5	Jannuzi/Burles	8312/7292	1860.7	3117.0	121	33	18
PG 1718+481	1.083	15.9	...	Burles	7292	1848.4	2672.7	81	15	14

^a S/N per pixel at 2382 Å and 2796 Å, ^b Total number of absorption features between Ly α and Ly β emission lines of quasar, ^c Number of identified metal absorption features between Ly α and Ly β emission lines of quasar, ^d Number of Galactic metal absorption features in entire observed wavelength region, ^e Coordinate of this quasar: RA: 13:19:56.3 Dec: +27:28:09 (J2000.0).

Table 2. Detected Transitions

Transition	λ_{rest}^a (Å)	Oscillator Strength ^a
Ly α	1215.6701	0.416400
H I λ 1026	1025.7223	0.079120
H I λ 972	972.5368	0.029000
H I λ 950	949.7431	0.013940
H I λ 938	937.8035	0.007799
H I λ 931	930.7483	0.004814
H I λ 926	926.2257	0.003183
H I λ 923	923.1504	0.002216
H I λ 921	920.9631	0.001605
H I λ 919	919.3514	0.00120
C I λ 1158	1157.910	0.021780
C I λ 1189	1188.833	0.016760
C I λ 1277	1277.245	0.096650
C I λ 1329	1328.833	0.058040
C II λ 1036	1036.3367	0.1231
C II λ 1335	1335.31	0.127
C II* λ 1336b	1335.6627	0.01277
C III λ 977	977.020	0.7620
C IV λ 1548	1548.195	0.190800
C IV λ 1551	1550.770	0.095220
N I λ 1134b	1134.1653	0.01342
N I λ 1135	1134.9803	0.04023
N I λ 1201	1200.7098	0.04423
N II λ 1084	1083.990	0.1031
N V λ 1239	1238.821	0.157000
N V λ 1243	1242.804	0.078230
O VI λ 1032	1031.927	0.132900
O VI λ 1038	1037.616	0.066090
Mg I λ 2853	2852.964	1.810000
Mg II λ 2796	2796.352	0.6123
Mg II λ 2803	2803.531	0.3054
Al II λ 1671	1670.787	1.880000
Al III λ 1855	1854.716	0.539000
Si II λ 990	989.873	0.133000
Si II λ 1190	1190.416	0.250200
Si II λ 1193	1193.290	0.499100
Si II* λ 1195	1194.500	0.623300
Si II λ 1260	1260.422	1.007000
Si II λ 1304	1304.370	0.147300
Si II λ 1527	1526.707	0.11600
Si III λ 1207	1206.500	1.660000
Si IV λ 1394	1393.755	0.528000
Si IV λ 1403	1402.770	0.262000
P II λ 1153	1152.818	0.236100
S II λ 1251	1250.584	0.005453
Cr II λ 2056	2056.254	0.1403
Cr II λ 2062	2062.234	0.1049
Cr II λ 2066	2066.161	0.06982
Mn II λ 2577	2576.877	0.3508
Mn II λ 2594	2594.499	0.2710
Mn II λ 2606	2606.461	0.1927
Fe I λ 2524	2523.608	0.279000
Fe II λ 1608	1608.4449	0.055450
Fe II λ 2250	2249.8768	0.00182
Fe II λ 2261	2260.7805	0.00244
Fe II λ 2344	2344.214	0.109700
Fe II λ 2374	2374.4612	0.02818
Fe II λ 2383	2382.765	0.3006
Fe II λ 2587	2586.650	0.064570
Fe II λ 2600	2600.1729	0.22390
Zn II λ 2063	2062.664	0.252900

^a These numbers are from Verner et al. (1996).

Table 3. Sample – Features with 5σ Identified in the *HST*/STIS E230M Spectra of 8 Quasars

#	λ_{obs}	W_{obs}	$\sigma(W_{obs})$	S	Line ID	z	Notes
PG 0117 + 213 ($z_{em} = 1.493$)							
1	2278.83	0.21	0.02	9.5	H λ 972	1.3430	
2	2285.29	0.97	0.04	25.7	C $\text{III}\lambda$ 977	1.3390	
3	2287.19	0.11	0.02	6.3	Ly α ?	0.8814	
4	2288.62	1.62	0.03	49.4	C $\text{III}\lambda$ 977	1.3430	Probable blend with Ly α at $z=0.8026$?
5	2292.90	0.14	0.02	7.9	Ly α ?	0.8861	
6	2293.51	0.14	0.02	6.8	Ly α ?	0.8866	
7	2295.47	0.47	0.02	21.4	H λ 938	1.4478	
8	2301.45	1.31	0.05	28.4	Ly α ?	0.8932	Reddest component is H λ 950 at $z=1.4242$
9	2306.53	0.05	0.01	4.2	Ly α ?	0.8973	
10	2306.91	0.20	0.01	13.9	C $\text{II}\lambda$ 1335	0.7290	
11	2307.52	0.18	0.02	11.8	C $\text{II}\lambda$ 1335	0.7290	
12	2311.85	0.76	0.04	21.2	H λ 1026	1.2543	
13	2313.76	0.51	0.02	20.9	Ly α ?	0.9033	
14	2316.57	0.09	0.01	6.0	Ly α ?	0.9056	
15	2318.26	0.04	0.01	5.5	Ly α ?	0.9070	Small contribution from N $\text{III}\lambda$ 989 at $z=1.3430$
16	2319.01	0.38	0.02	17.5	Ly α ?	0.9076	
17	2320.72	0.83	0.03	33.0	H λ 972	1.3866	
18	2321.88	0.11	0.01	9.3	H λ 931	1.4949	
19	2322.47	0.13	0.02	6.9	Ly α ?	0.9104	
20	2324.65	0.46	0.02	21.8	H λ 950	1.4478	
21	2325.78	0.06	0.01	5.5	Ly α ?	0.9132	
22	2331.23	0.04	0.01	3.0	H λ 972	1.3983	
23	2332.47	0.37	0.02	16.4	H λ 972	1.3983	
24	2334.98	0.19	0.02	10.1	Ly α ?	0.9207	
25	2339.13	0.40	0.03	12.7	H λ 938	1.4949	
26	2342.22	0.08	0.01	5.5	Ly α ?	0.9267	
27	2343.96	0.77	0.02	35.2	Fe $\text{II}\lambda$ 2344	0	
28	2349.69	0.53	0.02	24.8	Fe $\text{II}\lambda$ 2374	0	
29	2352.69	0.14	0.02	9.0	Ly α ?	0.9353	
30	2353.30	0.08	0.02	5.2	H λ 972	1.4242	
31	2357.58	0.38	0.02	16.9	Ly α ?	0.9393	
32	2359.25	0.34	0.03	13.5	Ly α ?	0.9407	
33	2369.23	0.35	0.02	18.1	H λ 950	1.4949	Blend to the red with C $\text{III}\lambda$ 977 at $z=1.4242$
34	2374.49	0.99	0.03	31.7	Fe $\text{II}\lambda$ 2374	0	
35	2380.41	0.66	0.02	27.7	H λ 972	1.4478	

Table 4. Detection Rate of Important Transitions

Transition	$\#_{cov}^a$	$\#_{det}^b$	Detection Rate ^c (%)
C $\text{II}\lambda$ 1335	27	15	56
C $\text{III}\lambda$ 977	26	13	50
C $\text{IV}\lambda$ 1548	26	23	88
N $\text{II}\lambda$ 1084	31	1	3
N $\text{V}\lambda$ 1239	37	9	24
O $\text{VI}\lambda$ 1032	30	27	90
Al $\text{II}\lambda$ 1671	18	7	39
Al $\text{III}\lambda$ 1855	10	2	20
Si $\text{II}\lambda$ 1260	36	13	36
Si $\text{III}\lambda$ 1207	36	21	58
Si $\text{IV}\lambda$ 1394	26	13	50
Fe $\text{II}\lambda$ 1608	22	2	9

^a Number of systems in which transition is covered, ^b Number of systems in which transition is detected, ^c Probability that transition is detected at $> 5\sigma$ for system in which it is covered.

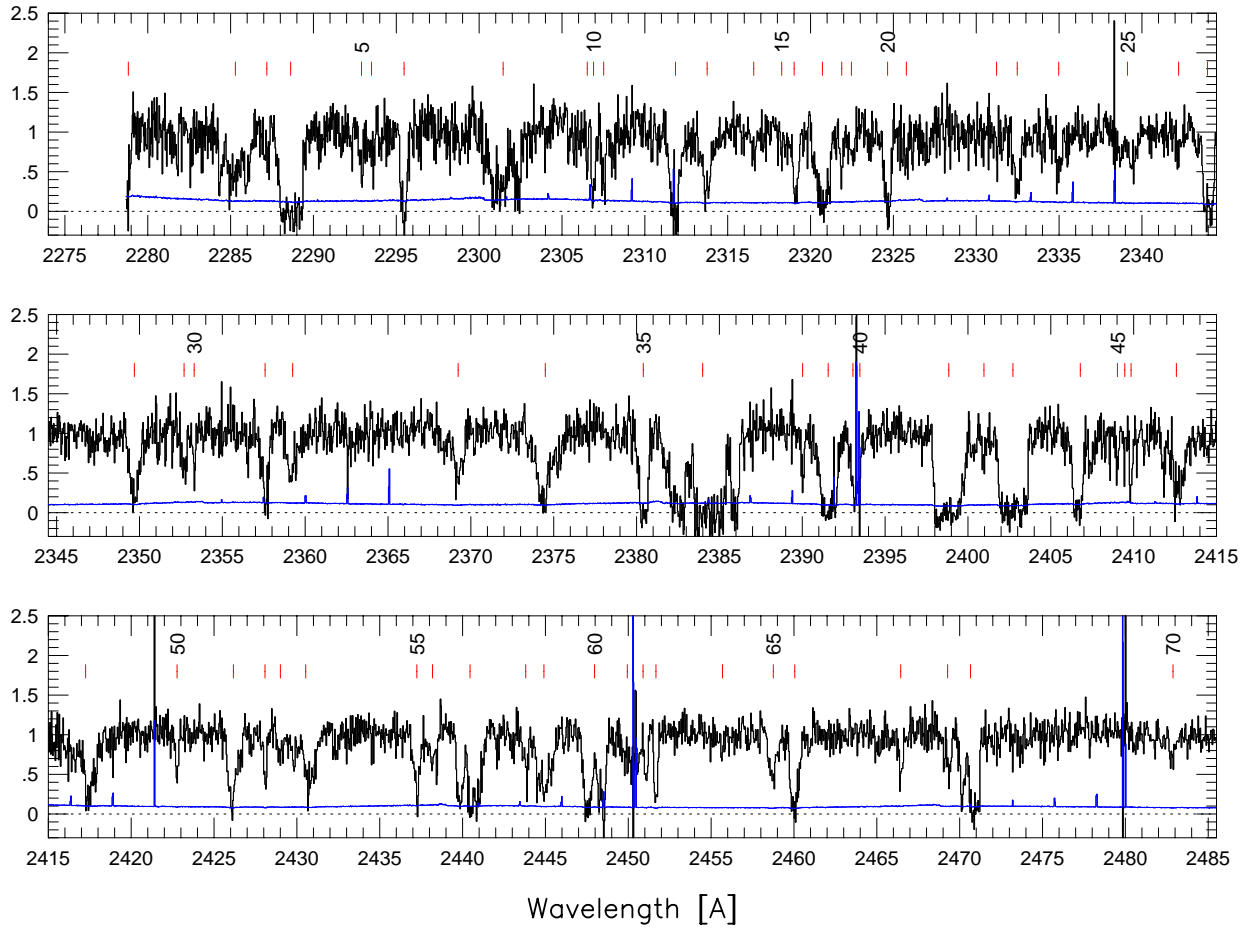


Figure 1a. Sample – Normalized flux versus wavelength for a portion of the *HST*/E230M spectrum of quasar PG0117 + 213. This is an example of a set of figures for all quasars and all wavelength coverage, which are given in the electronic version. The histogram displayed beneath the data represents the error spectrum. For reference, a dotted line is drawn at zero flux. Numbered ticks mark spectral features detected at a 5 σ level. These are listed in Table 3.

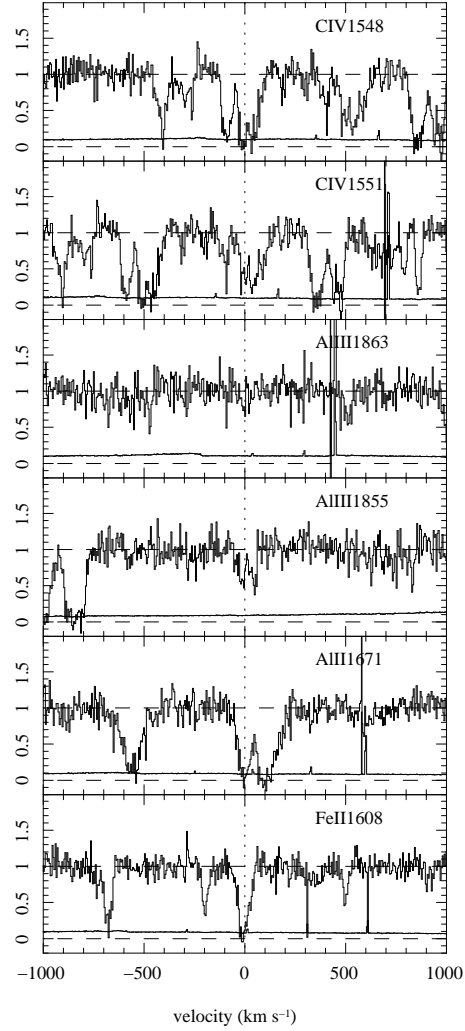


Figure 9. Sample – System plot for the $z = 0.5764$ system toward PG0117+213. Important transitions are plotted, unless they are so badly compromised by a blend that no useful constraints can be gathered. The transitions are aligned in velocity space, with 0 km s^{-1} corresponding to $z=0.5764$. The error spectrum is plotted beneath the data, and a dashed line shown at zero flux.